

# MEMS Resonators That Are Robust to Process-Induced Feature Width Variations

Rong Liu, Brad Paden, *Senior Member, IEEE*, and Kimberly Turner, *Member, IEEE*

**Abstract**—A stability analysis and design method for MEMS resonators is presented. The frequency characteristics of a laterally vibrating resonator are analyzed. With the fabrication error on the sidewall of the structure being considered, the first and second order frequency sensitivities to the fabrication error are derived. A simple relationship between the proof mass area and perimeter, and the beam width, is developed for single material structures, which expresses that the proof mass perimeter times the beam width should equal six times the area of the proof mass. Design examples are given for the single material and multi-layer structures. The results and principles presented in the paper can be used to analyze and design other MEMS resonators. [705]

**Index Terms**—Frequency stability, MEMS resonator, process variation.

## I. INTRODUCTION

RESONATORS have been widely used as a key component in MEMS devices, such as in microgyroscopes [1]–[3], microvibromotors [4], microengines [5], and RF systems [6]. Resonators are actuated, usually electrostatically, to oscillate at their natural resonant frequency, so that the robustness of the design frequency to process variations is one of the most important functional properties for the resonator design. Frequency stability of a resonator can directly affect the quality of the system in which it serves as a component. For the lateral vibrating rate gyroscopes, the frequency matching for their two vibrating modes is important for the output sensitivity. If frequency of any one of the modes shifts, the output signal's accuracy will be decreased. Although symmetry in these gyroscopes helps the two modes to track to first order, it is useful to enhance the frequency matching by designing the resonant frequency to be insensitive to process variations.

In microvibromotors, several resonators impact a bar to make it move in the plane of the chip. If the impacting frequencies of the resonators are not harmonic, the motion of the bar will be unpredictable. Similarly, two orthogonal resonators actuate the previously mentioned microengine, and the rotational stability of the engine is affected by the synchrony of these two resonators. Finally, in RF systems, the resonator is used in oscillators and filters. Therefore the frequency stability of the resonator in these applications is particularly important as its frequency determines the system performance in a fundamental way.

Fabrication processes induce wafer to wafer as well as on-wafer frequency variations. To identify sources of variability, one looks to the associated MEMS processes such as plasma-enhanced chemical vapor deposition (PECVD), lithography, reactive ion etch (LRIE), isotropic etch, deep reactive ion etch (DRIE), and sputter metallization. Process temperature variations have a critical influence in most of these processes. Wafer-to-wafer variations depend on the temperature control of process equipment and thermal stabilization of equipment prior to use. Thermally induced on-wafer variations are caused by wafer edge effects, process chamber asymmetry, and gas flow effects. Once processing begins, surface stresses disturb wafer planarity, which, in turn, affects optical lithographic steps and on-wafer device uniformity. Transport processes are difficult to control for uniformity both on-wafer and for matching devices. Application of photo resist, the distribution of process gasses, and the diffusion of reactant in wet etching are nearly impossible to control across a wafer, and wafer to wafer variations also occur. Pressure variation in gas-phase reactions is yet another source of process variability and the list goes on.

Thus, with present micromachining techniques, the fabrication process variation in MEMS is inevitable and it will continue to be the case when devices are miniaturized to the point of process limitations. For example, the fabrication tolerance for the width of a typical suspension beam is reported to be about 10% in [10]. Although it is known that the fabrication errors affect the frequency stability [9], [11], it may be that design for process variation was largely overlooked because of the structure complexity and differences in micromachining methods. The fabrication errors not only change the stiffness of the beam of the resonator, but also change the mass of the proof-mass. Even the same fabrication errors will cause different frequency variations for different resonator structures. In this paper, the frequency robustness for a folded-beam lateral vibrating resonator is analyzed. Based on the analysis, an optimum design method is presented for the resonator to obtain minimum frequency sensitivity. A simple relationship between the area and perimeter of proof mass and beam width is derived for single material structures.

## II. ANALYSIS OF A FOLDED-BEAM SUSPENDED RESONATOR WITH SINGLE STRUCTURAL MATERIAL

A folded-beam suspended resonator is shown in Fig. 1, where the cross section of the beams is assumed to be rectangular. The

Manuscript received June 4, 2001; revised April 5, 2002. Subject Editor R. T. Howe.

The authors are with the University of California at Santa Barbara, Santa Barbara, CA 93106 USA.

Digital Object Identifier 10.1109/JMEMS.2002.803279.

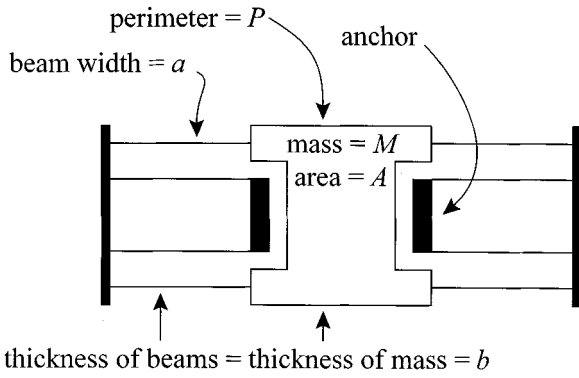


Fig. 1. Folded-beam suspended resonator.

merits of this kind of resonator include a wide frequency separation between the desired mode of oscillation and higher frequency parasitic modes, insensitivity to axial residual stress in the beam, and a smaller size than cantilevered beam resonators.

One objective of this paper is to derive a simple relationship between the design parameters to ensure low sensitivity to photolithographic- and etch-induced variations in line-width.

The lateral spring constant of the eight combined folded beams is given by

$$k = \frac{2a^3bE}{L^3} \quad (1)$$

where  $a$  and  $b$  are the width and thickness of the beams, respectively,  $L$  is the length of each beam, and  $E$  is the modulus of elasticity of the beam material.

The natural frequency of the resonator can be expressed as

$$\omega_0 = \sqrt{\frac{k}{M_{\text{eff}}}} = \sqrt{\frac{2a^3bE}{M_{\text{eff}}L^3}} \quad (2)$$

where,  $M_{\text{eff}}$  is the effective mass including the proof mass and an equivalent mass contributed by the folded-beam. Assuming that the thickness of the mass (in the dimension normal to the chip) is the same as that of the beams and that the structure consists of only one material, we have

$$M_{\text{eff}} = \rho b A_{\text{eff}} = \rho b(A + 8\mu La) \quad (3)$$

where  $A_{\text{eff}}$  is the effective area;  $\rho$  is the density of the material,  $A$  is the area of the proof mass excluding cut-outs, etc.,  $\mu$  is the mass equivalence coefficient (0.38 for folded-beam [6]). Presently, most proof masses are rectangular plates with attached comb-drive fingers and are solid or trussed.

Substituting (3) into (2) yields the natural frequency of the resonator

$$\omega_0 = \sqrt{\frac{2a^3E}{\rho A_{\text{eff}}L^3}} \quad (4)$$

In computing (4),  $b$  is cancelled because it appears both in the numerator and in the denominator. This shows that when the thickness of beam is the same as that of the moving mass the natural frequency of the system is independent of the thickness.

Hence it is reasonable to assume that the fabrication error is only on the "sidewalls" of the structure, i.e., there is a small

width error  $\delta$  in the lateral dimensions of the folded-beam and proof mass. (It is shown in the Appendix that our results hold for arbitrary "sidewall" errors.) Then the natural resonant frequency becomes

$$\omega_0(\delta) = \sqrt{\frac{2(a+2\delta)^3E}{\rho A_{\text{eff}}(\delta)L^3}} \quad (5)$$

where  $A_{\text{eff}}(\delta) = A(\delta) + 8\mu L(a+2\delta)$ , the approximation  $\delta \ll L$  is used to simplify the influence of  $\delta$  on the length of the beams, and  $L$  is held constant in the following derivations.

Therefore the first order sensitivity of  $\omega_0$  with respect to  $\delta$  is given as

$$\frac{\partial \omega_0}{\partial \delta} = 3\sqrt{\frac{2(a+2\delta)E}{\rho A_{\text{eff}}(\delta)L^3}} - \frac{1}{2}\sqrt{\frac{2(a+2\delta)^3E}{\rho A_{\text{eff}}(\delta)^3L^3}} \frac{\partial A_{\text{eff}}(\delta)}{\partial \delta} \quad (6)$$

It is easily obtained that the derivative of the area  $A$  with respect to the sidewall fabrication error  $\delta$  is directly proportional to the perimeter of the area in question including the perimeter of enclosed holes and voids. That is

$$\frac{\partial A_{\text{eff}}(\delta)}{\partial \delta} = P_{\text{eff}}(\delta) = P(\delta) + 16\mu L \quad (7)$$

where  $P(\delta)$  is the perimeter of the proof mass.

Substituting (7) into (6) yield

$$\frac{\partial \omega_0}{\partial \delta} = \left( 3 - \frac{(a+2\delta)[P(\delta) + 16\mu L]}{2A_{\text{eff}}(\delta)} \right) \sqrt{\frac{2(a+2\delta)E}{\rho A_{\text{eff}}(\delta)L^3}} \quad (8)$$

The second order sensitivity of  $\omega_0$  with respect to  $\delta$  can be derived as

$$\frac{\partial^2 \omega_0}{\partial \delta^2} = \left( 3 - \frac{3P_{\text{eff}}(\delta)(a+2\delta)}{A_{\text{eff}}(\delta)} - \frac{4(a+2\delta)^2}{A_{\text{eff}}(\delta)} + \frac{3(P_{\text{eff}}(\delta))^2(a+2\delta)^2}{4(A_{\text{eff}}(\delta))^2} \right) \sqrt{\frac{2E}{(a+2\delta)\rho A_{\text{eff}}(\delta)L^3}} \quad (9)$$

To set  $(\partial \omega_0)/(\partial \delta)$  and  $(\partial^2 \omega_0)/(\partial \delta^2)$  equal zero, the following conditions must be satisfied

$$\left. \frac{\partial \omega_0}{\partial \delta} \right|_{\delta} = 3A_{\text{eff}}(\delta) - \frac{1}{2}P_{\text{eff}}(\delta)(a+2\delta) = 0 \quad (10)$$

$$\left. \frac{\partial^2 \omega_0}{\partial \delta^2} \right|_{\delta} = 3 \left[ A_{\text{eff}}(\delta) - \frac{1}{2}P_{\text{eff}}(\delta)(a+2\delta) \right]^2 - 4A_{\text{eff}}(\delta)(a+2\delta)^2 = 0 \quad (11)$$

Setting  $\delta$  equal zero, and substituting (6) and (7) into (10) and (11) yield

$$\left. \frac{\partial \omega_0}{\partial \delta} \right|_{\delta=0} = 3A - \frac{1}{2}Pa + 16\mu La = 0 \quad (12)$$

$$\left. \frac{\partial^2 \omega_0}{\partial \delta^2} \right|_{\delta=0} = 3 \left[ A - \frac{1}{2}Pa \right]^2 - 4(A + 8\mu La)a^2 = 0 \quad (13)$$

If the parameters of the structure are designed to satisfy the (12) or, better yet, both (12) and (13), the frequency variation due to process variations can be reduced significantly.

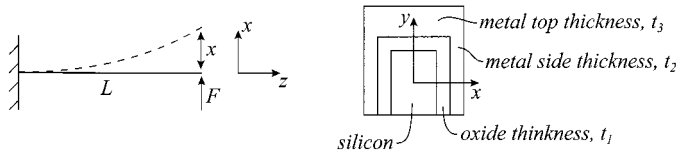


Fig. 2. Cantilever beam coated with two added material layers.

However, it is not usually the case that both (12) and (13) can be satisfied, as substituting (12) into (13) yields

$$3A + 24\mu L a = a^2 \quad (14)$$

$$\frac{1}{2}P + 8\mu L = a. \quad (15)$$

Generally, the width of the beam is small, and to satisfy both (14) and (15) the area and perimeter of the proof mass have to be less than  $a^2/3$  and  $2a$  respectively, which is unreasonable for most MEMS resonators. Therefore, only the first order sensitivity of  $\omega_0$  with respect to  $\delta$  can be designed to be zero in most cases. When the area of the proof mass is much larger than the area of the beam, (12) reduces to a convenient rule of thumb: “the perimeter of the proof mass times the beam width should be roughly six times the area of the proof mass. i.e.,  $Pa \approx 6A$ .”

### III. ANALYSIS FOR MULTILAYER STRUCTURES

For the sake of electrical conductivity, beams and proof masses in MEMS resonators are sometimes coated with other layers. For example, structures fabricated with SCREAM process [12] are coated with two material layers—one oxide layer with thickness  $t_1$  and one metal layer with side-thickness  $t_2$  and top-thickness  $t_3$ , as shown in Fig. 2.

The moment of inertia of the oxide layer and metal layer are given respectively by

$$I_{c1} = \frac{(a + 2t_1)^3(b + t_1) - a^3b}{12} \quad (16)$$

$$I_{c2} = \frac{(a + 2(t_1 + t_2))^3(b + t_1 + t_3) - (a + 2t_1)^3(b + t_1)}{12} \quad (17)$$

Because the coat-layers and the innermost silicon beam have the same lateral deflection  $\Delta X$  on the tip of the beam, the following expression can be given as

$$\Delta X = \frac{F_1 L^3}{3E_{c1} I_{c1}} = \frac{F_2 L^3}{3E_{c2} I_{c2}} = \frac{F_3 L^3}{E a^3 b} \quad (18)$$

where  $F$  is overall force on the tip of the beam;  $F_1, F_2, F_3$  are the forces of  $F$  on the oxide layer, metal layer and silicon beam, respectively.  $E_{c1}, E_{c2}$  and  $E$  are the Young’s modulus for three materials.

Defining the effective beam width, effective beam thickness and effective Young’s modulus, respectively, as

$$\begin{aligned} a_{\text{eff}} &= (a + 2(t_1 + t_2)) \\ b_{\text{eff}} &= (b + t_1 + t_3) \\ E_{\text{eff}} &= E_{c2} - \frac{(E_{c2} - E_{c1})(a + 2t_1)^3(b + t_1)}{(a + 2(t_1 + t_2))^3(b + t_1 + t_3)} \\ &\quad - \frac{(E_{c1} - E)a^3b}{(a + 2(t_1 + t_2))^3(b + t_1 + t_3)} \end{aligned} \quad (19)$$

(18) becomes

$$\Delta X = \frac{4FL^3}{E_{\text{eff}} a_{\text{eff}}^3 b_{\text{eff}}}. \quad (20)$$

If the fabrication errors occur only on innermost silicon beam, e.g.,  $a$  becomes  $a + 2\delta$ , then the sensitivity of effective elastic modulus can be simply expressed as

$$\begin{aligned} \frac{\partial E_{\text{eff}}}{\partial \delta} &= \frac{-12(E_{c2} - E_{c1})(a + 2\delta + 2t_1)^2(b + t_1)t_2}{(a + 2\delta + 2(t_1 + t_2))^4(b + t_1 + t_3)} \\ &\quad - \frac{12(E_{c1} - E)(a + 2\delta)^2b(t_1 + t_2)}{(a + 2\delta + 2(t_1 + t_2))^4(b + t_1 + t_3)}. \end{aligned} \quad (21)$$

If  $t_1$  and  $t_2$  are much smaller than the width of the beam, it can be assumed that the effective Young’s modulus remains constant in the frequency sensitivity analysis. In this case, the first and second sensitivities to the fabrication errors are similar to resonators that are not coated.

When there are fabrication errors in the lateral dimension of the layered materials, the effective modulus of elasticity will change too. Although the computation of sensitivities is straight-forward using computational algebra software such as Mathematica or Matlab, it is not useful to include the general output of such calculation here. An example will be given in Section IV-B.

Besides the above deformation equations, the mass of the proof mass will also have different expressions than that for a single material structure. The expression is dependent on construction, trussed or solid, of the proof mass, and will be given in the following section.

### IV. EXAMPLE OF A ROBUST DESIGN

#### A. Single Material Structure

A proposed structure for a resonator design is shown in Fig. 3. The trussed comb-driven mass is suspended by two symmetric folded-beams. The trussed structure for the mass simplifies the under-releasing of the structure from the substrate in, for example, the SCREAM process. Also, in some designs (not ours), it is useful that the truss will decrease the squeeze-film damping when there is a vertical vibration [11].

The proof mass is divided by row and column walls into smaller squares of dimension  $(k \times k)$ , except for the rightmost or leftmost sub-regions which are rectangles of dimension  $1/2k \times k$ . The width of all the walls in the trussed proof mass is  $t$ ; the number of row and column walls on the proof mass not including the outside walls are  $M$  and  $N$  respectively; the width and length of the comb fingers are  $d$  and  $g$  respectively, and the number of combs on each side is  $n_f$ . The four connectors that connect the folded beams to the proof mass are solid rectangles with width  $p$  and length  $q$ .

The design task is to specify the above parameters in addition to the folded-beam parameters  $L$  and  $a$ , and the structure thickness  $b$ , so that the natural resonant frequency of the structure equals  $\omega_0$  and its first order sensitivity to sidewall fabrication error is zero.

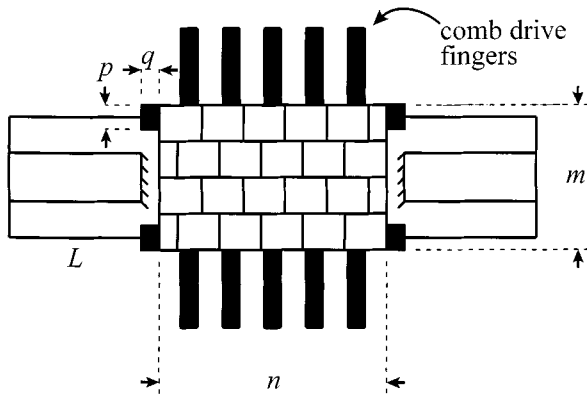


Fig. 3. Folded-beam suspended comb-drive resonator, where  $L$  is the length of each beam, proof mass width  $m$  comprises  $M + 2$  row walls, and length  $n$  comprises  $N + 2$  column walls.

The dimension  $k$  of the inner square satisfies

$$k = \frac{n - (N + 2)t}{N + 1/2} = \frac{m - (M + 2)t}{M + 1}. \quad (22)$$

The solid area on the proof mass can be expressed as

$$A = 2n_f dg + 4pq + nm - [n - (N + 2)t][m - (M + 2)t] \quad (23)$$

where  $2n_f dg$  is the area of the comb finger;  $4pq$  is the area of four connectors;  $nm$  is the overall area of rectangular proof mass;  $[n - (N + 2)t][m - (M + 2)t]$  is the total area of all inner trussed squares.

The overall perimeter of the proof mass is given by

$$P = 4n_f g + 4(2q - a) + 2(n + m) + 2(M + 1) \times [n - (N + 2)t] + 2(N + 1)[m - (M + 2)t]. \quad (24)$$

Substituting (23) and (24) into (4), (12) and (13) can yield a set of equations (the algebra is omitted as it is straight-forward). These equations plus (22) can be regarded as constraint conditions for solving for the structural parameters. The number of parameters is much larger than the number of equations, so that these equations are under-defined and there is some design freedom.

Practically, the parameters  $L$  and  $m$  can be initially given based on overall dimensional requirement of the whole device. The width  $p$  and length  $q$  of the connectors can also be given as a function of folded beam width. According to the designed electrostatic force, the size of the comb finger can be determined, which include  $d$ ,  $n_f$  and  $g$ . Since the total width of the fingers and gaps can not exceed the length of the device, a constraint condition has to be added as

$$2n_f d < n \quad (25)$$

$t$  can be initially given. After the above 8 parameters ( $L, m, t, d, n_f, g, p, q$ ) are determined, there are still four parameters ( $a, n, M, N$ ) to be resolved with (4), (12)–(14).

Rather than going through a complete design process involving detailed electrostatic design, etc., these eight parameters are set to typical values found in the literatures. Table I shows these parameters and material constants of silicon.

TABLE I  
SOME DESIGN PARAMETERS AND CONSTANTS

	Variable	Value
Predetermined parameters	$L$	$500\mu\text{m}$
	$m$	$350\mu\text{m}$
	$p$	$8\mu\text{m}$
	$q$	$10\mu\text{m}$
	$t$	$1\mu\text{m}$
	$n_f$	$30$
	$d$	$4\mu\text{m}$
Material constants	$g$	$30\mu\text{m}$
	$\rho$	$2330\text{kg/m}^3$
	$E$	$190\text{GPa}$

The natural frequency of the resonator is selected to be 5.5 KHz, which is in the range of typical MEMS resonator frequencies. So the angular frequency is  $\omega_0 = 34560$  (rad/s).

From (4), (14) and (15), the beam width for first- and second-order insensitivity can be initially calculated to be

$$a = \frac{\omega_0^2 L^3 \rho}{6E} = 3.05 \times 10^{-4} \mu\text{m} \quad (26)$$

which is too small for current MEMS fabrication technologies. Even though the width can be increased by increasing the beam length and natural frequency, the increase is limited and not sufficient to make the width consistent with current fabrication methods. Therefore, as mentioned previously, satisfying both the first- and second-order sensitivity conditions is practically impossible. When only the first condition is considered, the width of the folded beam can be set to  $4\mu\text{m}$ . Hence, the solid area and perimeter can be calculated by solving (4) and (12)

$$A = \frac{2a^3 E}{\omega_0^2 L^3 \rho} - 8\mu L a = 6.38418 \times 10^4 \mu\text{m}^2 \quad (27)$$

$$P = \frac{12a^2 E}{\omega_0^2 L^3 \rho} - 16\mu L = 1.02 \times 10^5 \mu\text{m}. \quad (28)$$

Now that the required area and perimeter of the proof mass are determined, solving (16)–(18) with respect to variables  $m, M$  and  $N$  yields  $n = 391\mu\text{m}$ ,  $N = 79.6$ , and  $M = 88.8$ .

Because both  $N$  and  $M$  must be integers, the  $N$  and  $M$  in (26) are rounded to 80 and 89 respectively. Then  $t, l$ , and  $m$  should be adjusted to satisfy (16)–(18), as  $t = 0.999\mu\text{m}$ ,  $n = 390\mu\text{m}$ , and  $m = 350\mu\text{m}$ .

From (16), the width of the inner square can be calculated as

$$k = \frac{n - (N + 2)t}{(N + 1/2)} = 3.33 \mu\text{m}. \quad (29)$$

## B. Multilayer Structure

In this subsection we outline the design of a multi-layer structure. The design steps are similar to the single material design except for different expressions of design conditions.

The top-view of the multilayer structure is same as Fig. 3. From (20), the lateral spring constant of the folded beams

$$k_{\text{eff}} = \frac{2a_{\text{eff}}^3 b_{\text{eff}} E_{\text{eff}}}{L^3}. \quad (30)$$

The natural frequency of the resonator can be expressed as

$$\omega_0 = \sqrt{\frac{k_{\text{eff}}}{M_{\text{eff}}}} = \sqrt{\frac{2a_{\text{eff}}^3 b_{\text{eff}} E_{\text{eff}}}{M_{\text{eff}} L^3}} \quad (31)$$

where  $M_{\text{eff}}$  is the effective mass comprising the mass of the proof mass  $M_{\text{proof}}$  plus an equivalent mass due to the folded beam  $M_{\text{beam}}$

$$M_{\text{eff}} = M_{\text{proof}} + \mu M_{\text{beam}}. \quad (32)$$

From the construction, the mass  $M_{\text{proof}}$  and  $M_{\text{beam}}$  can be expressed respectively as

$$\begin{aligned} M_{\text{proof}} &= 4q\{pb\rho + t_1(2b + p + 2t_1)\rho_1 \\ &\quad + [2t_2(b + t_1) + t_3(p + 2(t_1 + t_2))]\rho_2\} \\ &\quad + 2n_{fg}\{db\rho + t_1(2b + d + 2t_1)\rho_1 \\ &\quad + [2t_2(b + t_1) + t_3(d + 2(t_1 + t_2))]\rho_2\} \\ &\quad + \{2m + N[m - (M + 2)(t + 2(t_1 + t_2))]\} \\ &\quad + (M + 2)[n - 2(t + 2(t_1 + t_2))]\} \\ &\quad \times \{tb\rho + t_1(2b + t + 2t_1)\rho_1 \\ &\quad + [2t_2(b + t_1) + t_3(t + 2(t_1 + t_2))]\rho_2\} \\ M_{\text{beam}} &= 8L\{ab\rho + t_1(2b + a + 2t_1)\rho_1 \\ &\quad + [2t_2(b + t_1) + t_3(a + 2(t_1 + t_2))]\rho_2\}. \quad (33) \end{aligned}$$

The fabrication error here is assumed to occur only on the sidewalls of the innermost silicon structure, i.e., there is a small width error  $\delta$  in the lateral dimension of all innermost silicon components of the folded-beam and proof mass. There are no errors in the thickness. Then the natural resonant frequency becomes

$$\omega_0(\delta) = \sqrt{\frac{2(a_{\text{eff}} + 2\delta)^3 b_{\text{eff}} E_{\text{eff}}(\delta)}{M_{\text{eff}}(\delta) L^3}}. \quad (34)$$

Therefore the first order sensitivity of  $\omega_0$  with respect to  $\delta$  can be given as

$$\begin{aligned} \frac{\partial \omega_0}{\partial \delta} &= 3\sqrt{\frac{2(a_{\text{eff}} + 2\delta)b_{\text{eff}}E_{\text{eff}}(\delta)}{M_{\text{eff}}(\delta)L^3}} \\ &\quad + \frac{1}{2}\sqrt{\frac{2(a_{\text{eff}} + 2\delta)^3 b_{\text{eff}}}{E_{\text{eff}}(\delta)M_{\text{eff}}(\delta)L^3}} \frac{\partial E_{\text{eff}}(\delta)}{\partial \delta} \\ &\quad - \frac{1}{2}\sqrt{\frac{2(a_{\text{eff}} + 2\delta)^3 b_{\text{eff}}E_{\text{eff}}(\delta)}{M_{\text{eff}}(\delta)^3 L^3}} \frac{\partial M_{\text{eff}}(\delta)}{\partial \delta} \quad (35) \end{aligned}$$

where the  $(\partial M_{\text{eff}}(\delta))/(\partial \delta)|_{\delta=0}$  can be expressed as

$$\begin{aligned} \frac{\partial M_{\text{eff}}(\delta)}{\partial \delta} \Big|_{\delta=0} &= \{8q + 4n_{fg} + 2[(N + 2)m + (M + 2)n \\ &\quad - (N + 2)(M + 2)(t + 2(t_1 + t_2))] \\ &\quad - 16\mu L\}(b\rho + t_1\rho_1 + t_3\rho_2) \\ &\quad + 2[M + N + 4 - (N + 2)(M + 2)] \\ &\quad \times \{tb\rho + t_1(2b + t + 2t_1)\rho_1 \\ &\quad + [2t_2(b + t_1) + t_3(t + 2(t_1 + t_2))]\rho_2\}. \quad (36) \end{aligned}$$

So setting  $(\partial \omega_0)/(\partial \delta)|_{\delta=0} = 0$  yields

$$3M_{\text{eff}}E_{\text{eff}} + \frac{M_{\text{eff}}a_{\text{eff}}}{2} \frac{\partial E_{\text{eff}}(\delta)}{\partial \delta} \Big|_{\delta=0} - \frac{E_{\text{eff}}a_{\text{eff}}}{2} \frac{\partial M_{\text{eff}}(\delta)}{\partial \delta} \Big|_{\delta=0} = 0. \quad (37)$$

From (21),  $(\partial E_{\text{eff}}(\delta))/(\partial \delta)|_{\delta=0}$  can be expressed as

$$\frac{\partial E_{\text{eff}}}{\partial \delta} \Big|_{\delta=0} = \frac{-12(E_{c2} - E_{c1})(a + 2t_1)^2(b + t_1)t_2}{a_{\text{eff}}^4 b_{\text{eff}}} - \frac{12(E_{c1} - E)a^2 b(t_1 + t_2)}{a_{\text{eff}}^4 b_{\text{eff}}} \quad (38)$$

On the proof mass, the inner square condition becomes

$$\begin{aligned} k &= \frac{n - (N + 2)(t + 2(t_1 + t_2))}{N + 1/2} \\ &= \frac{m - (M + 2)(t + 2(t_1 + t_2))}{M + 1} \quad (39) \end{aligned}$$

From the above analysis, when the multilayer structure resonator is designed, three constraint conditions, i.e., (31), (37) and (39), should be satisfied. The design processes are similar to those of the single material structure resonator. Most of the design parameters are determined empirically based on process induced design rules. Only three variables are left to solve the above three (31), (37), and (39).

In the case of multi-layer structures, if other fabrication errors, such as thickness errors and coated-layer fabrication errors, are considered, the analysis and design methods are similar to the above analysis, but there is no pedagogical benefit in including the algebra here. With these fabrication errors being considered, the natural vibrating frequency of the designed resonator will be robust.

## V. CONCLUSION

In this paper, the frequency sensitivity characteristics of micro-resonators are analyzed, and a method to make the frequency robust to fabrication error of line width variation is presented.

For a resonator fabricated with only one material, the first- and second-order sensitivities of frequency to the linewidth fabrication error were derived. With the assumption of the beam and proof mass having the same thickness, the natural frequency is independent of the thickness, so that the thickness fabrication error can be ignored when considering the frequency sensitivity.

When both the first- and second-order sensitivities are set to zero, the dimensions of the resonator design become unreasonable (excessively wide beam and excessively small proof mass). Therefore, only the first-order sensitivity is considered in the design example. A rule of thumb for robust resonator design is that the proof mass perimeter times the beam width should be six times the area of the proof mass.

For the multilayer structure, its effective modulus of elasticity and mass are given, and its first order frequency sensitivity to the sidewall fabrication error of the innermost beam is derived. The results can be used to analyze the effect of other fabrication errors on the structure.

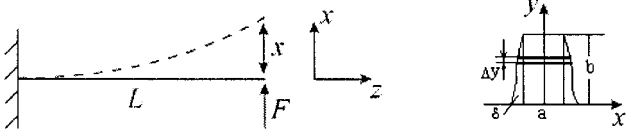


Fig. 4. Cantilever beam and its cross section with arbitrary sidewall fabrication error.

The concepts presented here can be applied to more complex systems using numerical optimization or computer algebra software such as Mathematica or Matlab.

#### APPENDIX

##### EQUATIONS FOR MEMS RESONATOR WITH ARBITRARY PROFILE OF SIDEWALL FABRICATION ERROR

From the cross section of the beam (see Fig. 4), a thin segment of thickness  $\Delta y$  is considered. If  $\Delta y$  is small enough, this segment can be regarded as a rectangle in the dimension of  $\Delta y \times (a + 2\delta_i)$ .  $\delta_i$  is the fabrication error on the segment, and is dependent on the position of the segment on the cross-section. This segment with length of  $L$  is a thin beam. The tip deflection of this thin beam can be expressed as

$$\Delta X_i = \frac{4F_i L^3}{E[a + 2\delta_i]^3 \Delta y} \quad (\text{A-1})$$

where the  $F_i$  is the force on the tip of this thin beam.

The whole beam can be divided into many thin beams as above. Because the overall force on the tip of the beam  $F = \sum_i F_i$ , and any tip deflection of those thin beams is equal to tip deflection of the whole beam, i.e.,  $\Delta X = \Delta X_i$ , the deformation equation of the whole beam can be given as

$$\Delta X = \frac{4FL^3}{E \int_0^b [a + 2\delta(y)]^3 dy}. \quad (\text{A-2})$$

Then the elastic coefficient of the beam can be obtained as

$$k = \frac{E \int_0^b [a + 2\delta(y)]^3 dy}{4L^3}. \quad (\text{A-3})$$

The mass of a unit length of beam can be expressed as

$$\begin{aligned} M_{\text{unit}} &= \rho \int_0^b [a + 2\delta(y)] dy \\ &= \rho b(a + 2\delta_{\text{mean}}) \end{aligned} \quad (\text{A-4})$$

where  $\delta_{\text{mean}} = (\int_0^b \delta(y) dy) / (b)$  is the mean fabrication error on one side of the beam. Equation (A-4) has the same form as that for a beam with line-width fabrication error, except the constant  $\delta$  for with line-width fabrication error beam is replaced with  $\delta_{\text{mean}}$ . So the mass of the proof mass which can be obtained similarly as  $\delta_{\text{mean}}$  is considered as the mean fabrication error on the width of all structures.

$$M = \rho b A(\delta_{\text{mean}}) \quad (\text{A-5})$$

where  $A(\delta_{\text{mean}})$  is the area of the proof mass with fabrication error.

The natural frequency of the folded beam suspended resonator can be given as

$$\begin{aligned} \omega_0 &= \sqrt{\frac{2E \int_0^b [a + 2\delta(y)]^3 dy}{b\rho A(\delta_{\text{mean}})L^3}} \\ &= \sqrt{\frac{2Eb(a + 2\delta_{\text{mean}})^3 + 2E \left[ 12a \left( \int_0^b \delta(y)^2 dy - \delta_{\text{mean}}^2 b \right) \right]}{b\rho A(\delta_{\text{mean}})L^3}} \\ &\quad + \frac{8 \left( \int_0^b \delta(y)^3 dy - \delta_{\text{mean}}^3 b \right)}{b\rho A(\delta_{\text{mean}})L^3} \quad (\text{A-6}) \end{aligned}$$

Because the following equations are satisfied

$$2E \left[ 12a \left( \int_0^b \delta(y)^2 dy - \delta_{\text{mean}}^2 b \right) + 8 \left( \int_0^b \delta(y)^3 dy - \delta_{\text{mean}}^3 b \right) \right] \Big|_{\delta=0} = 0 \quad (\text{A-7})$$

$$\frac{\partial 2E \left[ 12a \left( \int_0^b \delta(y)^2 dy - \delta_{\text{mean}}^2 b \right) + 8 \left( \int_0^b \delta(y)^3 dy - \delta_{\text{mean}}^3 b \right) \right]}{\partial \delta_{\text{mean}}} \Big|_{\delta=0} = 0 \quad (\text{A-8})$$

where  $\delta = 0$  means that the fabrication error on every point on the side-wall is set theoretically to zero. Then the first sensitivity of the natural frequency to the mean fabrication error can be expressed as

$$\frac{\partial \omega_0}{\partial \delta_{\text{mean}}} \Big|_{\delta=0} = \frac{3 \sqrt{\frac{2(a + 2\delta_{\text{mean}})E}{\rho A(\delta_{\text{mean}})L^3}}}{-\frac{1}{2} \sqrt{\frac{2(a + 2\delta_{\text{mean}})^3 E}{\rho A(\delta_{\text{mean}})^3 L^3}} \frac{\partial A(\delta_{\text{mean}})}{\partial \delta_{\text{mean}}}} \Big|_{\delta_{\text{mean}}=0} \quad (\text{A-9})$$

From (A-9), the same results can be obtained as in (12) with  $\delta$  in (12) replaced by  $\delta_{\text{mean}}$ .

#### REFERENCES

- [1] W. C. Tang, M. G. Lim, and R. T. Howe, "Electrostatic comb drive levitation and control method," *J. Microelectromech. Syst.*, vol. 1, no. 4, pp. 170–178, Dec. 1992.
- [2] Y. Mochida, M. Tamura, and K. Ohwada, "A micromachined vibrating rate gyroscope with independent beams for the Drive and detection modes," in *Tech. Dig. IEEE Int. Conf. MEMS'99*, 1999, pp. 618–623.
- [3] L. A. Yeh, H. Jiang, and N. C. Tien, "Integrated polysilicon and DRIE bulk silicon micromachining for an electrostatic torsional actuator," *J. Microelectromech. Syst.*, vol. 8, no. 4, pp. 456–465, Dec. 1999.
- [4] M. J. Daneman, N. C. Tien, O. Solgaard, A. P. Pisano, K. Y. Lau, and R. S. Muller, "Linear microvibromotor for positioning optical components," *J. Microelectromech. Syst.*, vol. 5, no. 3, pp. 159–165, Sept. 1996.
- [5] L. A. Romero, F. M. Dickey, and S. C. Holswade, "A method for achieving constant rotation rates in a microorthogonal linkage system," *J. Microelectromech. Syst.*, vol. 9, no. 2, pp. 236–244, June 2000.
- [6] H. J. De Los Santos, *Introduction to Microelectromechanical (MEM) Microwave System*. Dedham, MA: Artech House, 1999.
- [7] Y. K. Yong and J. R. Vig, "Resonator surface contamination—A cause of frequency fluctuation?," *IEEE Trans. Ultrason., Ferroelectr., Freq. Contr.*, vol. 36, no. 4, pp. 452–458, July 1989.
- [8] T. B. Gabrielson, "Mechanical—Thermal noise in micromachined acoustic and vibration sensors," *IEEE Trans. Electron Devices*, vol. 40, no. 5, pp. 903–909, May 1993.
- [9] F. E. H. Tay, J. Xu, Y. C. Liang, V. J. Logeeswaran, and Y. F. Yao, "The effects of nonparallel plates in a differential capacitive microaccelerometer," *J. Microelectromech. Syst.*, vol. 9, pp. 283–293, 1999.

- [10] Y. S. Hong, J. H. Lee, and S. H. Kim, "A laterally driven symmetric micro-resonator for gyroscopic applications," *J. Micromech. Microeng.*, vol. 10, pp. 452–458, 2000.
- [11] J. B. Starr, "Squeeze-film damping in solid-state accelerometers," in *Solid-State Sensor and Actuator Workshop, Tech. Dig.*, New York, 1990, pp. 44–47.
- [12] K. A. Shaw, Z. L. Zhang, and N. C. MacDonald, "SCREAM-I, a single-mask single-crystal silicon, reactive ion etching process for microelectromechanical structures," *Sens. Actuators, Phys. A*, vol. 40, p. 63, 1994.



**Rong Liu** received the B.A. degree in mechanical engineering and the Ph.D. degree in mechanics from Beijing University of Aeronautics & Astronautics, China, in 1990 and 1996, respectively. He received the M.S. degree in mechanics from the Beijing Polytechnic University in 1993.

From 1996 to 1999, he has worked in Beijing University of Aeronautics & Astronautics, where his research focused on robotics. In 1999, he was with the City University of Hong Kong as an Associate Researcher for a cleaning robot project. From July 2000 to 2001, he was a Visiting Scholar at University of California, Santa Barbara, doing research in MEMS. He is currently working as an Associate Professor in Beijing University of Aeronautics & Astronautics.



**Brad E. Paden** (S'83–M'85–SM'02) received the Ph.D. degree in electrical engineering from University of California, Berkeley, in 1985.

He is currently a Professor at the University of California, Santa Barbara, in the Department of Mechanical and Environmental Engineering. His research interests focus on nonlinear control theory and its application to electromechanical systems. In 1988, he was a Visiting Fellow at the Department of Mathematics, University of Western Australia.

He has consulted for industry on numerous projects

including artificial heart design, maglev vehicle design, energy storage flywheels, and has served as an Associate Editor for the *Journal of Robotic Systems*. In 1992, he Co-Founded Magnetic Moments, LLC, a company specializing in magnetic bearing and electromechanical system design. He directs RoboChallenge, a robotics-based K-12 outreach program involving over 100 students in mobile robot design.

Prof. Paden was the recipient of the Best Paper Award from the *ASME Journal of Dynamic Systems, Measurement, and Control* in 1993, and the IEEE Control System Society Technology Award in 2001.



**Kimberly L. Turner** (M'01) received the B.S. degree in mechanical engineering from Michigan Technological University and the Ph.D. degree in theoretical and applied mechanics from Cornell University, Ithaca, NY, in 1994 and 1999, respectively.

She is currently an Assistant Professor of Mechanical Engineering at the University of California, Santa Barbara, a position she has held since July 1999. She is continuing her research in the areas of MEMS and nanosystems. Her interests involve many areas of micro- and nanosystems, especially

dynamics and characterization, and applications utilizing nonlinear dynamics. Some current projects in her research program include the development of parametrically resonant chemical sensors, coupled oscillator dynamics, mechanical filters, and nanoscale device fabrication and characterization. She holds one U.S. Patent and has three others pending.

Dr. Turner is the recipient of the 1997 Varian Fellowship Award given by the American Vacuum Society, as well as an NSF graduate research fellowship, and a 2001 NSF CAREER Award. Her work has been published in *Nature* and *Review of Scientific Instruments*, as well as other publications. She is an active Member of ASME, IEEE, as well as the American society for Engineering Education, the American Vacuum Society, Tau Beta Pi, Pi Tau Sigma, and the Cornell Society of Engineers.